Control Engineering Practice 19 (2011) 1459–1467

Contents lists available at SciVerse ScienceDirect

Control Engineering Practice

journal homepage: www.elsevier.com/locate/conengprac

Nested PID steering control for lane keeping in autonomous vehicles

Riccardo Marino [a], Stefano Scalzi [a,*], Mariana Netto [b]

[a] University of Rome Tor Vergata, Electronic Engineering Department - DIE, Via del Politecnico 1, 00133 Roma, Italy
[b] LCPC/INRETS, LIVIC Vehicle-Infrastructure-Driver Interactions Research Unit, 14 Route de la miniére, 78000 Versailles, France

ARTICLE INFO

Article history:
Received 12 November 2010
Accepted 18 August 2011
Available online 9 September 2011

Keywords:
Vehicle dynamics
Integrated automotive control
Lane keeping
Autonomous vehicles

ABSTRACT

In this paper a nested PID steering control in vision based autonomous vehicles is designed and experimentally tested to perform path following in the case of roads with an uncertain curvature. The control input is the steering wheel angle: it is designed on the basis of the yaw rate, measured by a gyroscope, and the lateral offset, measured by the vision system as the distance between the road centerline and a virtual point at a fixed distance from the vehicle. No lateral acceleration and no lateral speed measurements are required. A PI active front steering control based on the yaw rate tracking error is used to improve the vehicle steering dynamics. The yaw rate reference is computed by an external control loop which is designed using a PID control with a double integral action based on the lateral offset to reject the disturbances on the curvature which increase linearly with respect to time. The proposed control scheme leads to a nested architecture with two independent control loops that allows us to design standard PID controls in a multivariable context (two outputs, one input). The robustness of the controlled system is theoretically investigated with respect to speed variations and uncertain vehicle physical parameters. Several simulations are carried out on a standard big sedan CarSim vehicle model to explore the robustness with respect to unmodelled effects. The simulations show reduced lateral offset and new stable μ-split braking maneuvres in comparison with the model predictive steering controller implemented by CarSim. Finally the proposed control law is successfully tested by experiments using a Peugeot 307 prototype vehicle on the test track in Satory, 20 km west of Paris.

1. Introduction

Intelligent vehicles and automated highway systems have attracted a growing attention in the last years (as can be seen from the research activity overview presented in Shladover, 2007 and the progress done in the last decade as shown in Urmson, Duggins, Jochem, Pomerleau, & Thorpe, 2008) with the aim of increasing safety and comfort: see for instance Enache, Mammar, and Netto (2008, 2009), Raharijaona, Duc, and Mammar (2004), Kang, Hindiyeh, Moon, Gerdes, and Yi (2008), Cerone, Chinu, and Regruto (2002), Cerone, Milanese, and Regruto (2009), Hatipoglu, Redmill, and Özgüner (1997), MacAdam (1981), Falcone, Borrelli, Asgari, Tseng, and Hrovat (2007), Takahashi and Asanuma (2000), Broggi, Bertozzi, Fascioli, Lo Bianco, and Piazzi (1999), Foote et al. (2006), Montemerlo et al. (2006), Ackermann, Sienel, Steinhauser, and Utkin (1995), Liu, Nagai, and Raksincharoensak (2008), Baumgarten (2004) and Pauly and Baumgarten (2005). In Enache et al. (2008, 2009) a feedback from lateral and longitudinal vehicle speeds, yaw angle error and yaw rate is used to help the driver to steer the vehicle back to the lane during diminished driving capability due to inattention. The control strategy is based on the Lyapunov theory and LMI optimization by defining polytopic and hypercubic state space regions in which the driving task is considered safe; the main idea is to approximate these regions by standard and composite Lyapunov level curves. In Raharijaona et al. (2004) a H_∞ controller is designed to minimize the effect of the disturbances on the measured lateral offset and the desired yaw angle. In Kang et al. (2008) a steering controller, which uses finite preview optimal control methods, is proposed to control the measured lateral offset, the yaw angle and their derivatives. In Cerone et al. (2009) a closed loop control strategy which feeds back the lateral offset is proposed: an automatic lanekeeping is combined with the driver's steering with no need of switching strategies between the driver and the lane keeping control. In Cerone et al. (2002) a control system based on the loop shaping technique is tested by experiments using a feedback from the lateral offset. In Hatipoglu et al. (1997) a nonlinear observer based control strategy is investigated by measuring the lateral offset, its derivative, the yaw angle and the yaw rate. In MacAdam (1981) a model predictive steering controller is used to emulate the driver behavior in the CarSim environment: it is designed on the basis of a simplified linear model and on longitudinal and lateral speed, yaw

* Corresponding author. Tel.: +39 06 7259 7412.
E-mail address: scalzi@ing.uniroma2.it (S. Scalzi).

0967-0661/$ - see front matter © 2011 Elsevier Ltd. All rights reserved.
doi:10.1016/j.conengprac.2011.08.005

angle and yaw rate measurements to predict the error with respect to a given target path. Also in Falcone et al. (2007) a model predictive control approach is followed: the controlled outputs are the lateral offset, the yaw rate and the yaw angle; the controller is designed both on a nonlinear and a linear vehicle model using lateral and longitudinal vehicle speeds, yaw angle and yaw rate measurements. In Takahashi and Asanuma (2000) a feedforward and a feedback action on the lateral offset and the yaw angle error is experimented. In Broggi et al. (1999) a gain scheduling based proportional feedback from the lateral offset is experimented. In Foote et al. (2006) a feedforward term from road curvature and a PID based on a weighted sum of the heading error and the lateral offset are used as steering controller in the DARPA Grand Challenge. In the same competition the yaw angle and a nonlinear term proportional to the lateral offset are used in Montemerlo et al. (2006) to design the steering controller. Furthermore, to improve safety, driver comfort and vehicle performance, several driver assistance systems are investigated in the literature. In Liu et al. (2008) a steering assistance control system with a feedback from the lateral offset and lateral speed is designed to follow the desired path while an assistance torque is applied in order to improve the vehicle handling and steering feel. In Baumgarten (2004) and Pauly and Baumgarten (2005) the active front steering is proposed and implemented on BMW 5 Series vehicle. In Baumgarten (2004) a PI active front steering control based on the yaw rate tracking error with different gains for braked and unbraked driving condition is used while in Pauly and Baumgarten (2005) a patented method is proposed to ensure safety during active steering system failure computing the steering wheel angle as the sum of the proposed control and the driver steering action.

Most control algorithms employed in lane keeping make use of pole placement, model predictive and observer based techniques or require the difficult measurements of lateral speed, vehicle absolute position and orientation. The simplest algorithm (Broggi et al., 1999) only implements a proportional feedback from the lateral offset. Since in addition to lateral offset measurements from vision systems the yaw rate measurements are easily obtained by an on board gyroscope, in Ackermann et al. (1995) the steering angle time derivative is designed as a proportional feedback from the yaw rate in addition to a PIDD controller from the lateral offset measurements showing the obtained performance by simulations.

In this paper a new nested PID control scheme which integrates the active steering action based on the yaw rate error with the lane keeping action based on the lateral offset is proposed and tested by experiments (a preliminary work which did not include experiments and a complete robustness analysis has been presented in Marino, Scalzi, Netto, & Orlando, 2009). No lateral speed measurement is used since it can be hardly measured and, in addition, with high cost and low accuracy and reliability. A PI active front steering control based on the yaw rate tracking error is designed to reject constant disturbances and the effect of uncertain parameters while improving the vehicle steering dynamics; in order to integrate the additional lateral offset measure the yaw rate reference is viewed as the control signal in an external control loop; it is designed using a PID control (with an additive double integral action) on the lateral offset to reject the disturbances on the curvature which are assumed to increase linearly with respect to time. Also in Ackermann et al. (1995) the desired yaw rate reference signal r_d is first designed: an observer is used on the basis of both the yaw rate and the lateral offset which makes use of the look ahead distance while in this paper r_d is designed on the basis of lateral displacement measurements only leading to two independent nested control loops. Hence the proposed control scheme is called nested while the controller in Ackermann et al. (1995) is referred to as a cascaded control. The nested control structure with two independent control loops allows to design standard PID controls in a multivariable context (two outputs, one input). The design is inherently robust since it makes no use of system parameters (such as the look-ahead distance l_s) which are largely uncertain. The independence of the two control loops gives high flexibility: the outer loop can be switched from vision based autonomous to human driver without changing the beneficial inner loop. The overall control for the steering wheel angle is designed on the basis of the yaw rate measured by a gyroscope and the lateral offset measured by the vision system as the distance between the road centerline and a virtual point at a fixed distance from the vehicle. Sufficient conditions for robust stability of the controlled system, with respect to speed variation, look-ahead distance and uncertainties on vehicle physical parameters such as the front and rear cornering stiffnesses and the vehicle mass are given by using the theorem presented in Vidyasagar and Kimura (1986) and Paoletti, Grasselli, and Menini (2004). It is shown how the robustness of the controlled system decreases as speed increases as expected. The asymptotic stability is however ensured for all perturbations in the range of interest. Several simulations, such as the tracking of a CarSim environment default path and a standard sudden braking action on surfaces with different adherence conditions (μ-split braking manoeuvre), are carried out on a standard big sedan CarSim vehicle model to explore the robustness with respect to unmodelled effects, such as combined lateral and longitudinal tire forces, pitch and roll. The simulations show reduced lateral offset and new stable μ-split braking maneuvres with respect to the CarSim model predictive steering controller which requires lateral speed. Due to the good performances of the proposed control law, which are shown in the simulation section, a practical implementation has been successfully performed: a Peugeot 307 prototype vehicle has been used on the 3.4 km long test track located in Satory, 20 km west of Paris. The experimental setup and the track test results are described and illustrated in Section 5.

2. Vehicle model

A detailed standard big sedan CarSim vehicle model is used in numerical simulations to analyze the responses of both the uncontrolled and the controlled vehicle. The CarSim vehicle model uses nonlinear tire forces according to combined sideslip theory as described in Pacejka (2004), nonlinear spring models, and incorporates the major kinematics and compliance effects in the suspensions and steering systems including differential load transfer for each wheel. However, to design the controller, a widely used simplified single track vehicle model, shown in Ackermann (2002), is considered which captures the essential vehicle steering dynamics:

$$m(\dot{v}_x - r v_y) = f_{lf}\cos\delta_f - f_{sf}\sin\delta_f + f_{lr}$$

$$m(\dot{v}_y + r v_x) = f_{lf}\sin\delta_f + f_{sf}\cos\delta_f + f_{sr}$$

$$J\dot{r} = l_f(f_{lf}\sin\delta_f + f_{sf}\cos\delta_f) - l_r f_{sr} \tag{1}$$

$$f_{si}(\alpha_i) = D\sin\{C\,\mathrm{atan}[(1-E)B\alpha_i + E\,\mathrm{atan}(B\alpha_i)]\} \tag{2}$$

$$\alpha_f = \frac{v_y + l_f r}{v_x} - \delta_f, \quad \alpha_r = \frac{v_y - l_r r}{v_x} \tag{3}$$

where f_{si}, with $i=f,r$, are the front and rear lateral forces and f_{li}, $i=f,r$ are the front and rear longitudinal forces which are modelled according to the Pacejka tire model, as described in Pacejka (2004). The tire sideslip angle and consequently the sign of the lateral forces are computed as in (3) according to CarSim tire

Table 1
Vehicle nomenclature:

v	vehicle velocity
r	vehicle yaw rate
a_y	lateral acceleration
δ_p	driver steering angle
m	vehicle mass
l_f	front axle-CG dist.
l_s	look-ahead distance
$f_{l,s}$	log./lateral forces
$\alpha_{f,r}$	tire sideslip angle
$B_{f,r}$	Pacejka parameter
$D_{f,r}$	Pacejka parameter
$v_{x,y}$	long. lateral speed
β	vehicle sideslip angle
c_a	aerodynamic coeff.
δ_f	front steering angle
J	vertical axle inertia
l_r	rear axle-CG dist.
μ	adherence coefficient
ρ	road curvature
$c_{f,r}$	cornering stiffness
$C_{f,r}$	Pacejka parameter
$E_{f,r}$	Pacejka parameter

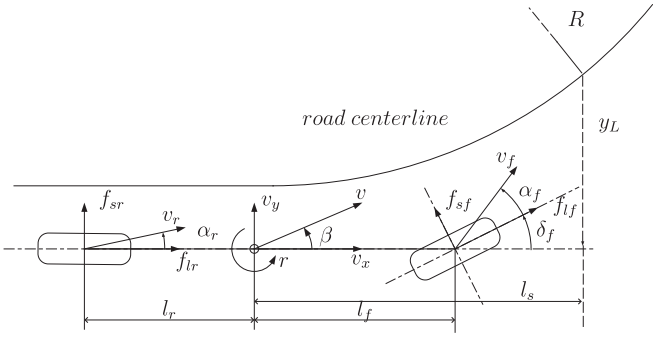

Fig. 1. Single track vehicle model.

model (SAE ISO standard, see Pacejka, 2004). All variables and parameters are defined in the Appendix (Table 1). The CCD camera measures the lateral deviation y_L from the centerline at a distance l_s from the vehicle; the y_L dynamics can be modeled as in Enache et al. (2009) as follows:

$$\dot{y}_L = \beta v + l_s r + v\psi \tag{4}$$

where ψ is the relative yaw angle, y_L is the lateral offset from the road centerline at a preview distance l_s (see Fig. 1) and β is the vehicle sideslip angle that can be computed from $v_y = v\sin\beta$ which becomes $v_y = v\beta$ considering small angle approximation. The system (1) is linearized about uniform rectilinear motion ($v_x = v =$ constant, $r=0$, $v_y=0$, $\delta_f = 0$): the longitudinal dynamics is decoupled from the lateral dynamics and can be neglected for control purposes. The reduced linear system, $\dot{x} = Ax + Bu$, which includes the lateral offset dynamics (4) is given by

$$\begin{bmatrix} \dot{\beta} \\ \dot{r} \\ \dot{\psi} \\ \dot{y}_L \end{bmatrix} = \begin{bmatrix} a_{11} & a_{12} & 0 & 0 \\ a_{21} & a_{22} & 0 & 0 \\ 0 & 1 & 0 & 0 \\ v & l_s & v & 0 \end{bmatrix} \begin{bmatrix} \beta \\ r \\ \psi \\ y_L \end{bmatrix} + \begin{bmatrix} b_1 \\ b_2 \\ 0 \\ 0 \end{bmatrix} \delta_f + \begin{bmatrix} 0 \\ 0 \\ -v \\ 0 \end{bmatrix} \rho \tag{5}$$

where ρ is the road curvature defined as $\rho = 1/R$, with R the curvature radius. The coefficients appearing in system (5), which may depend on v and on uncertain physical parameters are

$$a_{11} = -\frac{(c_f + c_r)}{mv}, \quad a_{12} = -1 - \frac{(c_f l_f - c_r l_r)}{mv^2}$$

Table 2
Vehicle parameters for the linear model (5).

m	2023 kg
l_f	1.26 m
c_f	2.864e+5 N/rad
J	6286 kg m^2
l_r	1.90 m
c_r	1.948e+5 N/rad

$$a_{21} = -\frac{(c_f l_f - c_r l_r)}{J}, \quad a_{22} = -\frac{(c_f l_f^2 + c_r l_r^2)}{Jv}$$

$$b_1 = \frac{c_f}{mv}, \quad b_2 = \frac{c_f l_f}{J} \tag{6}$$

where c_f and c_r are the front and the rear tire cornering stiffness which are the linear approximation of (2) and are related to the parameters in Pacejka's formula as follows:

$$c_f = B_f C_f D_f$$

$$c_r = B_r C_r D_r \tag{7}$$

The vehicle parameters for the simplified single track vehicle model (5), whose values are identified from a big sedan CarSim vehicle model, are given in Appendix (Table 2); since a lumped vehicle model is used the tire cornering stiffnesses shown in Table 1 are two times the cornering stiffnesses of the front and the rear CarSim vehicle wheels.

3. Control strategy

3.1. Control design

The proposed control strategy is illustrated in Fig. 2. It involves the design of two nested control blocks. The first one, called C_1, has to ensure the tracking of a yaw rate reference signal on the basis of the yaw rate tracking error in spite of constant disturbances and parameter uncertainties; the second one, called C_2, has to generate the yaw rate reference signal on the basis of the lateral offset in order to drive the lateral offset y_l to the desired lateral offset y_d which is equal to zero.

The task of C_1 is to steer to zero the difference between the measured yaw rate r and desired yaw rate r_d.

Following the active steering approach shown in Baumgarten (2004) a PI control has been used for C_1:

$$C1: \delta_f = -K_{P1}(r - r_d) - K_{I1}\int_0^t (r - r_d)\, dv = -K_{P1}(r - r_d) - K_{I1}\alpha_0 \tag{8}$$

where α_0 is the additional state introduced by the dynamic control (8). The feedback from the yaw rate r improves the transients by changing the eigenvalues displacement of the steering dynamics. Substituting (8) in (5) leads to the augmented vehicle state space description:

$$\dot{x}_{as} = \begin{bmatrix} a_{11} & a_{12} - K_{P1}b_1 & 0 & 0 & -b_1 K_{I1} \\ a_{21} & a_{22} - K_{P1}b_2 & 0 & 0 & -b_2 K_{I1} \\ 0 & 1 & 0 & 0 & 0 \\ v & l_s & v & 0 & 0 \\ 0 & 1 & 0 & 0 & 0 \end{bmatrix} x_{as} + \begin{bmatrix} K_{P1}b_1 \\ K_{P1}b_2 \\ 0 \\ 0 \\ -1 \end{bmatrix} r_d + \begin{bmatrix} 0 \\ 0 \\ -v \\ 0 \\ 0 \end{bmatrix} \rho \tag{9}$$

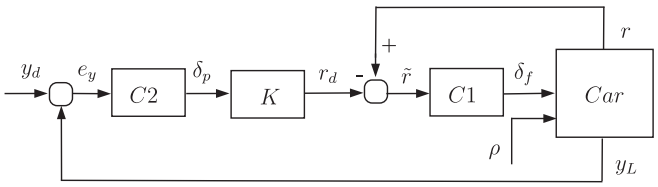

Fig. 2. Controlled system scheme.

where

$x_{as} = [\beta\ r\ \psi\ y_L\ \alpha_0]^T$.

Once the regulator C_1 is designed, the key idea is to integrate the additional lateral offset measure considering the yaw rate reference signal r_d in (9) as the control input to be designed to drive the output y_L to zero. Therefore, to design the desired yaw rate reference, it is necessary to model the dynamics of the road curvature, considering it as a disturbance on the lateral offset. In the case of a constant road curvature one integral term is needed to reject the disturbance. Road building standards define that the clothoids are to be used to interconnect straight roads to constant curvature roads and, at constant speed, this implies that the road curvature increases linearly with respect to time:

$$\rho = \frac{1}{F^2} q \tag{10}$$

where F is a fixed scale parameter and q is the length measured along clothoid which increases linearly at constant vehicle speed. Hence the road curvature may be considered as increasing linearly with respect to time. An additional integral term is necessary to obtain zero steady state tracking error and the regulator C_2 becomes

$$\begin{aligned} C2 : \delta_p &= -K_{P2} y_L - K_{I2} \int_0^t y_L\, dv \\ &\quad - K_{I3} \int_0^t \int_0^v y_L\, d\eta\, dv - K_d \dot{y}_{Ld} \\ &= -K_{P2} y_L - K_{I2} \alpha_2 - K_{I3} \alpha_1 - K_d \dot{y}_{Ld} \end{aligned} \tag{11}$$

where

$$\dot{\alpha}_1 = y_L \tag{12}$$

$$\dot{\alpha}_2 = \alpha_1 \tag{13}$$

and the signal y_{Ld} is given by

$$\dot{\alpha}_3 = -\frac{1}{\tau}\alpha_3 + y_L \tag{14}$$

$$y_{Ld} = -\frac{1}{\tau^2}\alpha_3 + \frac{1}{\tau} y_L \tag{15}$$

where τ is the filter time constant.

The final structure of the control algorithm is shown in Fig. 2 in which C_1 is given by (8), C_2 is given by (11)–(15) and the reference model for the linearized system is given by $r_d = K\delta_p$ in which K is a design parameter.

3.2. Control properties

To choose the seven control gains and the look-ahead distance the bandwidth of the transfer function between r_d and δ_f, of the closed loop linear system (9) and (11), is constrained to be about 10 Hz which is the actuator bandwidth in the experiments. The Simulink Response Optimization toolbox was used to tune the design parameters through numerical optimization: the design requirements are expressed in terms of rise time, settling time and overshoot on the response of the lateral deviation y_l to a unit step reference input y_d for the nonlinear vehicle model available by CarSim. The gains are obtained from a Sequential Quadratic Programming method as described in Gill, Murray, and Wright (1981). The rise time has been chosen according to the actual industrial steering actuator (also according to the available steering actuator in the LIVIC research center). Different optimization procedures (see for example Grassi et al., 2001 in which the parameters of the controller are tuned by a convex optimization algorithm, minimizing a weighted difference between the actual loop transfer function) can be used to maximize a performance index. The resulting control parameters are

$$K_{P1} = 20, \quad K_{I1} = 10, \quad K_{P2} = 30$$

$$K_{I2} = 0.01, \quad K_{I3} = 0.01, \quad K_d = 0.05 \tag{16}$$

while K (see Fig. 2) is chosen as

$$K = \lim_{s\to 0} C[sI - A]^{-1} B \tag{17}$$

in which

$$C = [0,\ 1,\ 0,\ 0] \tag{18}$$

and

$$B = [b_1,\ b_2,\ 0,\ 0]^T \tag{19}$$

with nominal parameters.

The controlled system (9) and (11)–(15) is then

$$\dot{x}_c = A_c x_c + B_c \rho \tag{20}$$

$$A_c = \begin{bmatrix} a_{c11} & a_{c12} & 0 & a_{c14} & a_{c15} & a_{c16} & a_{c17} & a_{c18} \\ a_{c21} & a_{c22} & 0 & a_{c24} & a_{c25} & a_{c26} & a_{c27} & a_{c28} \\ 0 & 1 & 0 & 0 & 0 & 0 & 0 & 0 \\ v & l_s & v & 0 & 0 & 0 & 0 & 0 \\ 0 & 1 & 0 & a_{c54} & 0 & a_{c56} & a_{c57} & a_{c58} \\ 0 & 0 & 0 & 1 & 0 & 0 & 0 & 0 \\ 0 & 0 & 0 & 0 & 0 & 1 & 0 & 0 \\ 0 & 0 & 0 & 1 & 0 & 0 & 0 & -\frac{1}{\tau} \end{bmatrix}$$

$$B_c = [0,\ 0,\ -v,\ 0,\ 0,\ 0,\ 0,\ 0]^T \tag{21}$$

with

$$x_c = [\beta,\ r,\ \psi,\ y_L,\ \alpha_0,\ \alpha_1,\ \alpha_2,\ \alpha_3]^T \tag{22}$$

and the equilibrium point x_{ce} is shown below:

$$x_{ce} = -\begin{bmatrix} \frac{(b_2 a_{12} - b_1 a_{22})v}{a_{11} b_2 - a_{21} b_1} \\ -v \\ \frac{(a_{42}(a_{11} b_2 - a_{21} b_1) + a_{41}(b_1 a_{22} - b_2 a_{12}))v}{a_{43}(a_{11} b_2 - a_{21} b_1)} \\ 0 \\ -\frac{(a_{11} a_{22} - a_{21} a_{12})v}{K_{I1}(a_{11} b_2 - a_{21} b_1)} \\ 0 \\ \frac{v}{K K_{I2}} \\ 0 \end{bmatrix} \rho, \tag{23}$$

where τ is set equal to $\tau = 0.01$ and l_s is chosen equal to $l_s = 12$ m while the parameters a_{cij} are shown in Table 3. Since the look-ahead distance varies due to road hills or bumps a robustness analysis is carried of in the related Section 3.3. With the chosen gains (16) the controlled system stability is guaranteed since the poles are on the left hand side of the complex plane. In addition, the stability will be proved to be robust with respect to vehicle parameter variations in the robustness analysis section. The frequency behavior of the controlled system (20) has been analyzed. In Fig. 3 the behavior of the controlled system with respect to the road curvature ρ is shown for an increasing speed ($v = [15,35]$ m/s).

Table 3
Substitutions.

$a_{c11}=a_{11}$	$a_{c12}=a_{12}-K_{P1}b_1$
$a_{c14}=-\frac{K_{P1}b_1K(K_{P2}\tau+K_d)}{\tau}$	$a_{c15}=-b_1K_{I1}$
$a_{c16}=-K_{P1}b_1KK_{I3}$	$a_{c17}=-K_{P1}b_1KK_{I2}$
$a_{c18}=\frac{K_{P1}b_1KK_d}{\tau^2}$	$a_{c21}=a_{21}$
$a_{c22}=a_{22}-K_{P1}b_2$	$a_{c24}=-\frac{K_{P1}b_2K(K_{P2}\tau+K_d)}{\tau}$
$a_{c25}=-b_2K_{I1}$	$a_{c26}=-K_{P1}b_2KK_{I3}$
$a_{c27}=-K_{P1}b_2KK_{I2}$	$a_{c28}=\frac{K_{P1}b_2KK_d}{\tau^2}$
$a_{c54}=K\frac{K_{P2}\tau+K_d}{\tau}$	$a_{c56}=KK_{I3}$
$a_{c57}=KK_{I2}$	$a_{c58}=-\frac{KK_d}{\tau^2}$

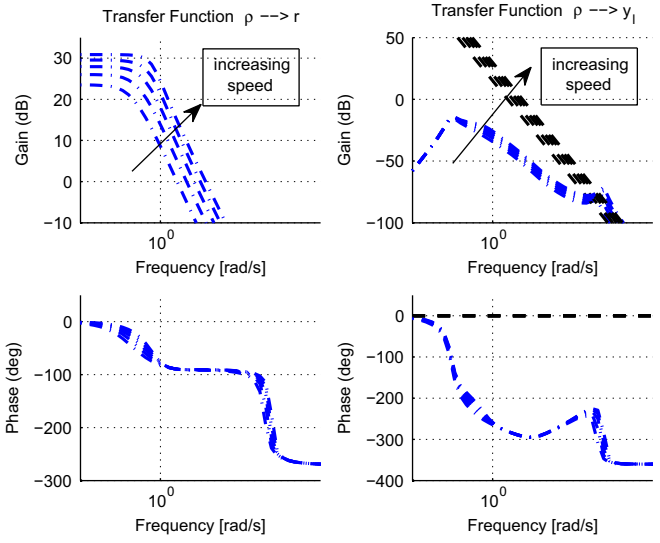

Fig. 3. Bode diagram of the transfer functions between ρ and r of the controlled system and Bode diagram of the transfer functions between ρ and y_L of the controlled system (dash-dot) and the uncontrolled system (dash-dash) for an increasing vehicle speed.

On the left hand side of Fig. 3 the transfer function from the road curvature to the yaw rate is shown while, on the right hand side of Fig. 3, the reduction of the road curvature effect on the lateral offset is shown with respect to the uncontrolled system. The transfer function between ρ and y_L for a speed v equal to $v=36$ m/s is computed below to show the double zeros at the origin which ensure the rejection of disturbances that increase linearly with respect to time (the remaining zeros are negative as can be also observed on the right hand side of Fig. 3):

$$y_L=-1296\frac{s^2(s+0.05)(s+6.69)(s+100)(s+1157)}{s^8+h_7s^7+h_6s^6+h_5s^5+h_4s^4+h_3s^3+h_2s^2+h_1s+h_0}\rho; \tag{24}$$

For completeness, the transfer functions between ρ and y_L of the uncontrolled system is reported below:

$$y_L=-\frac{v^2}{s^2}\rho \tag{25}$$

the coefficients h_i are shown in Table 4.

3.3. Robustness

Many variations may occur from the nominal vehicle parameters: the cornering stiffnesses may change due to different road adherence conditions and/or low tire pressure, the vehicle mass and moment of inertia change from unloaded to full load conditions; moreover the look-ahead distance can also vary due to road hills or bumps. To analyze the robustness of the proposed nested lane keeping approach the transfer function from the steering angle to the lateral offset is considered by varying the uncertain parameters of interest c_f, c_r, m and l_s for different values of the vehicle speed v; the considered parameters' variations also influence the inner loop and this has been taken into account in the following. The vehicle's moment of inertia variations are approximated taking into account the variations of the vehicle mass $J=l_fl_rm$.

Table 4
Substitutions.

$h_7=1251.7$	$h_6=7.4\times10^5$	$h_5=582\times10^5$	$h_4=3981\times10^5$
$h_3=11231\times10^5$	$h_2=7434\times10^5$	$h_1=1373\times10^5$	$h_0=1.3\times10^5$

The following definitions are used: Σ_0 as the closed loop system (20) with unperturbed parameters; Σ as the closed loop system with perturbations on c_f, c_r, m and l_s, $\Delta_P=P-P_0$ as the perturbation, where P and P_0 are the transfer functions of the perturbed and of the nominal vehicle model between the wheel angle δ_f and the lateral offset y_L respectively; V_0 as the control sensitivity function that is the transfer function between the control input δ_f and the given reference y_d; $\overline{\sigma}$ as the operator that gives the greater singular value of a transfer function. The following theorem (see Paoletti et al., 2004; Vidyasagar & Kimura, 1986) can be applied.

Theorem 1 (*Paoletti et al., 2004; Vidyasagar and Kimura, 1986*). *If*:

($\boldsymbol{\alpha}_0$) Σ_0 *is well-posed and asymptotically stable,*
($\boldsymbol{\alpha}_1$) $\overline{\sigma}[V_0(j\omega)]\le 1/l_a(\omega)\ \forall\omega\in\Re^+$,

then Σ *is asymptotically stable for all variations or perturbations of* P *from* P_0 *such that*:

($\boldsymbol{\beta}$) *the number of eigenvalues of* A *in* C^- *is equal to the number of eigenvalues of* A_0 *in* C^-,
($\boldsymbol{\gamma}$) Σ *is well-posed,*
($\boldsymbol{\delta}$) $\overline{\sigma}[\Delta_P(j\omega)]<l_a(\omega),\forall\omega\in\Re^+$,

where $l_a(\omega)$ *is a positive and continuous function of* $\omega\in\Re^+$. □

Given the control scheme in Fig. 2 the control sensitivity function can be computed as follows:

$$\delta_f=\frac{C_2KC_1}{1+C_1P_r}e_y \tag{26}$$

$$e_y=\frac{1}{1+C_2K\overline{P}_{L1}}y_d \tag{27}$$

so that

$$V_0=\frac{\delta_f}{y_d}=\frac{C_2KC_1}{(1+C_1P_r)(1+C_2K\overline{P}_{L1})} \tag{28}$$

in which P_r is the transfer function between δ_f and r of the system (5) under parameter variations

$$P_r=\frac{r}{\delta_f}=C(sI-A)^{-1}B \tag{29}$$

and $\overline{P}_{L1}$, which take into account the parameter variations also in the first internal loop, is the transfer function between r_d and y_L of the system (9)

$$\overline{P}_{L1} = \frac{y_L}{r_d} = \frac{C_1 P_y}{1 + C_1 P_r} \tag{30}$$

with

$$P_y = \frac{y_L}{\delta_f} = [0\ 0\ 0\ 1](sI - A)^{-1} B. \tag{31}$$

By choosing $l_a(\omega)$ equal to the inverse of $\overline{\sigma}[V_0(j\omega)]$, Theorem 1 is satisfied for different speeds and perturbations on the tire parameters such as the cornering stiffnesses c_r, c_f, the vehicle mass m and the look-ahead distance l_s. Considering a vehicle speed of $v = 20$ m/s and a perturbation of 30% with respect to the nominal parameters the hypothesis ($\boldsymbol{\delta}$) of the theorem is satisfied as shown in Fig. 4. By increasing the perturbation up to 40% the theorem does not ensure the asymptotic stability as shown in Fig. 5. For all the perturbations that satisfy the hypothesis ($\boldsymbol{\delta}$), the hypothesis ($\boldsymbol{\gamma}$) is satisfied since the system is well-posed: there is no direct connection between the input and the output signals of the system (5); moreover also the hypothesis ($\boldsymbol{\beta}$) is satisfied: the parameter variations only change the eigenvalues (λ_1,λ_2) of the steering dynamics (β,r) since the system (5) is lower triangular

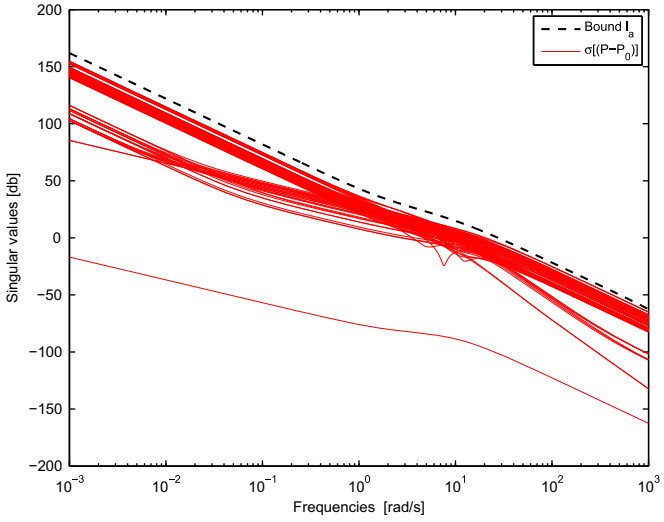

Fig. 4. Singular values analysis at a vehicle speed of $v = 20$ m/s and a perturbation of 30%.

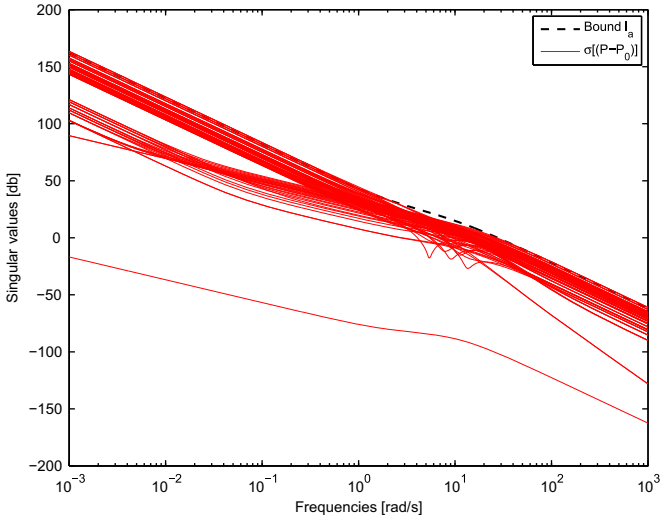

Fig. 5. Singular values analysis at a vehicle speed of $v = 20$ m/s and a perturbation of 40%.

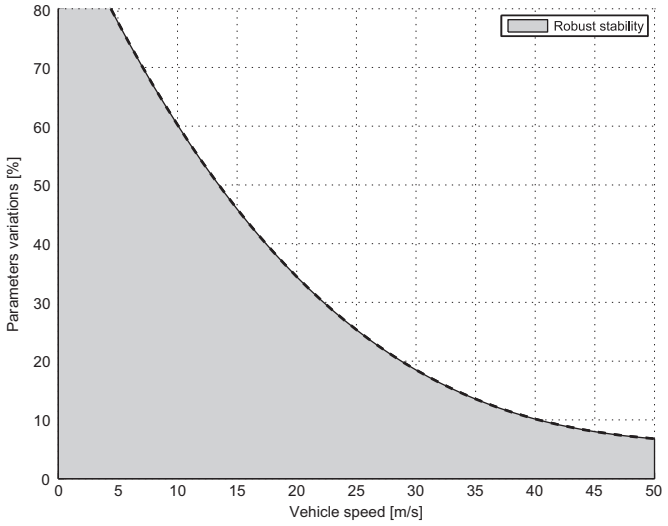

Fig. 6. Robustness with respect to parameter variations for increasing speed.

and, in addition, these changes modify λ_1,λ_2 so that they always belong to the left complex plane for the perturbations range that satisfy the hypothesis ($\boldsymbol{\delta}$). On the Y-axis of Fig. 6 the percentage of variation of all the parameters c_r, c_f, m and l_s for which the Theorem is satisfied for different speeds is shown. The robustness decreases as the speed increases as shown in Fig. 6, in which a speed variation from 1 m/s to 50 m/s is considered; the asymptotic stability of Σ is guaranteed by the theorem for all the area under the curve of Fig. 6 in which the hypothesis ($\boldsymbol{\beta}$), ($\boldsymbol{\gamma}$) and ($\boldsymbol{\delta}$) are satisfied. However the above-mentioned theorem gives only sufficient conditions and after some simulations performed on wet road, it is reasonable to think that the effective robustness may be greater than the robustness guaranteed by the theorem. Moreover it is interesting to observe that when the theorem fails it is due to the cornering stiffness and/or the vehicle mass while the control stability is really robust with respect to the look-ahead distance. This property is important in the test track especially in the case of road bumps and in the case in which the image processing algorithms are not able to perform the path following at the chosen look-ahead distance; in this case the algorithm provides a new look-ahead distance according to Labayrade, Ieng, & Aubert (2004, 2006) while the control is robust with respect to this variations.

4. CarSim simulations

Several simulations in the CarSim environment have been performed to compare the proposed nested PID control with the CarSim driver model (designed to emulate an average driver) which is based on a model predictive control system designed in MacAdam (1981) and makes also use of state feedback: vehicle lateral speed and yaw rate. Moreover the performed simulations with the CarSim big sedan vehicle are performed to evaluate the robustness with respect to the neglected dynamics and the performances with respect to vehicle time varying parameters since, due to the load transfer for instance, the cornering stiffness varies. The CarSim vehicle model uses detailed nonlinear tire models according to combined slip theory and takes into account the major kinematics and compliance effects of the suspensions (nonlinear spring models) and steering systems. The vehicle has a nonlinear, second order, speed depending rack and pinion ratio steering system; for the active steering a realistic actuator with a bandwidth of 10 Hz is considered. The first simulation, shown in

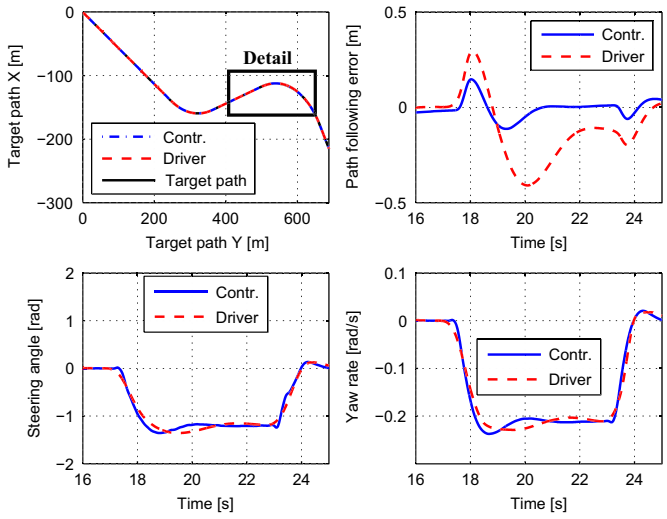

Fig. 7. Standard CarSim path following maneuvre ($v=30$ m/s).

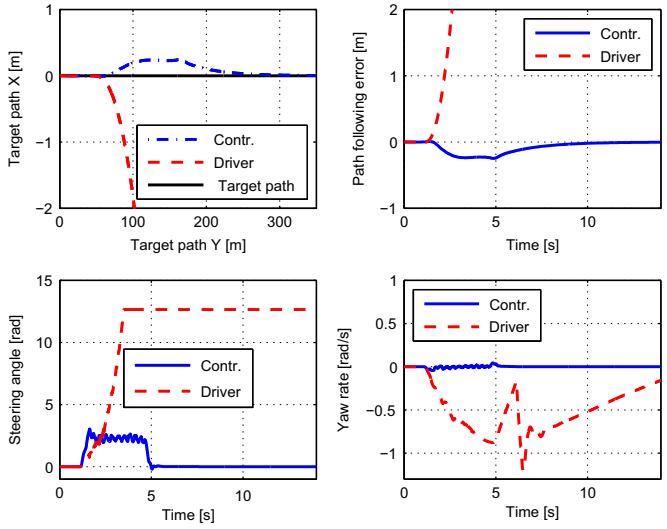

Fig. 8. μ-split braking maneuvre.

Fig. 7, concerns a path following in the case of a typical highway road curvature profile at a vehicle speed of 30 m/s. In Fig. 7 the *XY*-trajectory, the path following error, the steering angle and the yaw rate are shown for the vehicle controlled by the CarSim driver model and by the proposed control. To emphasize the simulation results only a detail of the path following maneuvre is depicted as shown in the top-left subplot of Fig. 7: in that curve the vehicle reaches a lateral acceleration of 7.8 m/s^2. Both controllers achieve the path following; however, as shown in the top-right subplot of Fig. 7, a more accurate lane keeping and a reduced path following maximum error in the lateral direction of 70% are obtained by the proposed control law.

To analyze the performance of the proposed controlled system with respect to tire-road adherence variations a μ-split braking maneuvre is performed ($\mu=0.1$ on the left hand side and $\mu=0.8$ on the right hand side in the CarSim model). A sudden braking action of 15 MPa at a velocity of 40 m/s is given on both the vehicle with the MPC and the vehicle with the nested PID control strategy: the proposed control system ensures the lane keeping (top-left subplot of Fig. 8) while the vehicle controlled by the CarSim driver model leaves the lane. The CarSim steering action saturates at the maximum allowed mechanical constraint that is equal to 720° (12.56 rad in Fig. 8) while small oscillations on the steering signal provided by the proposed control, due to the ABS that prevents wheel lock while ensuring greater decelerations can be observed (bottom-left subplot of Fig. 8). In this situation the proposed feedback on the yaw rate error, which has a faster dynamics with respect to the lateral offset dynamics, really improve the performance of the overall proposed control system. The maneuvre shown in Fig. 8 has been performed with the same MPC controller, which has been used to emulate the driver in the CarSim framework, and with the proposed lane keeping controller without any change in the control parameters.

5. Test track and experimental setup

Experimental tests were conducted on the test track located in Satory, 20 km west of Paris, France. The track is 3.5 km long with various road profiles including a straight lane and tight bends (see Fig. 9). The experimental vehicle, a Peugeot 307, was equipped with an inertial system that makes use of MEMS-based gyroscopes and accelerometers (Crossbow IMU440) which is used to measure the yaw rate; the vehicle speed is measured by the Hall sensors mounted on the four wheels and a Trimble GPS is used to describe the position of the vehicle in the track. The steering angle has been obtained from an optical encoder. The look-ahead lateral offset is measured by means of a front view camera installed on the top-middle of the windshield; the look-ahead distance has been fixed to 12 m according to the performed analysis and the computed simulations. This camera can detect the lane markers using image processing algorithms and provides the lateral offset (see Labayrade et al., 2004, 2006). In the case in which image processing algorithms is not able to perform the path following at the chosen look-ahead distance the algorithm provides a new look-ahead distance according to Labayrade et al. (2004, 2006). The proposed control is able to achieve good results also in spite of variations on l_s as computed from the robust analysis with respect to l_s and as shown by the test track. The vehicle is equipped with a 48 V electric drive d.c. motor mounted on the steering wheel which is mechanically connected to the wheel. The controller is written in C code and runs at 10 ms, and on a PC equipped with an AMD Athlon 2.0 GHz processor. The lateral offset is available with a sampling time of 40 ms. Sensors, PC and the actuator communicate through CAN bus, Ethernet and RS232.

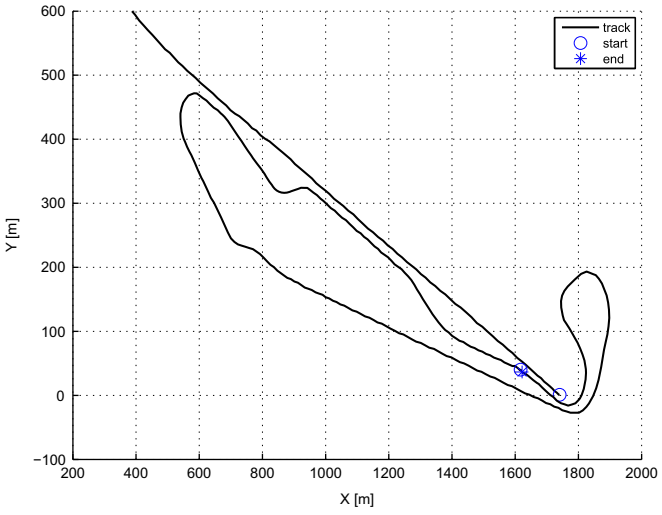

Fig. 9. Paris test track.

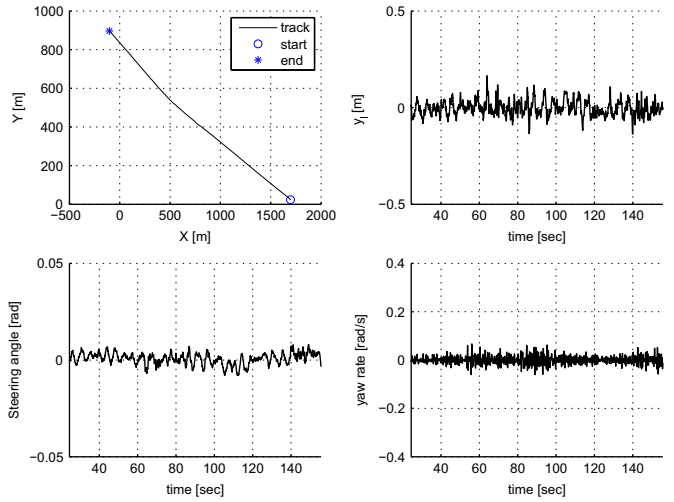

Fig. 10. Straight line following maneuvre performed by the Peugeot 307 on the test track ($v \in [20-25]$ m/s).

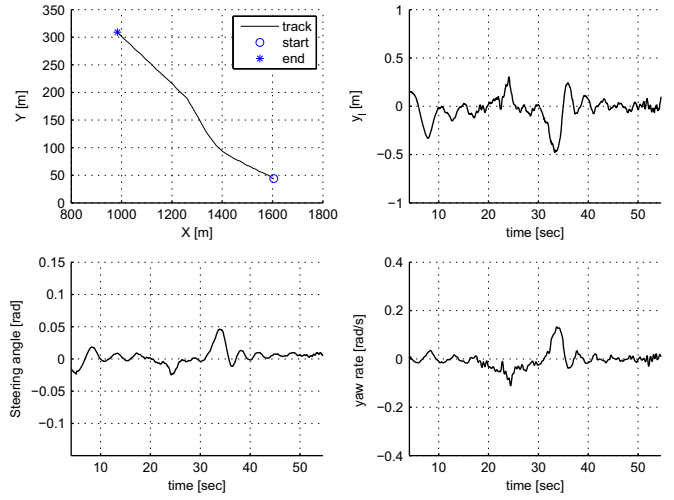

Fig. 11. Path following maneuvre performed by the Peugeot 307 on the test track ($v \in [14-16]$ m/s).

The first test is performed on the straight road. In Fig. 10 the *XY*-trajectory, the path following error, the steering angle and the yaw rate measured by the experimental vehicle are shown. The control, shown in the bottom-left subplot, is able to keep the lane while compensating the effects of road bank angles and very small changes in the road direction performing a very small lane keeping error as shown in the top-right subplot.

The second test is performed on the curved road shown in the top-left subplot of Fig. 11 with a maximum road curvature of about 0.01 (1/m). The control is activated at $t=8$ s by the driver through a button while he was driving the vehicle from 0 to 8 s. The control is able to keep the vehicle within the lane performing a maximum lateral error of 0.5 m as shown in the top-right subplot of Fig. 11.

The third test is performed on a more demanding section of the test track which is shown in the top-left subplot of Fig. 12 with a maximum road curvature of about 0.015 (1/m). The control, shown in the bottom-left subplot, is deactivated at $t=174$ s by the driver since not all the test track is equipped for lane keeping. The control is able to keep the vehicle within the lane performing a maximum lateral error of 0.6 m as shown in the top-right subplot of Fig. 12.

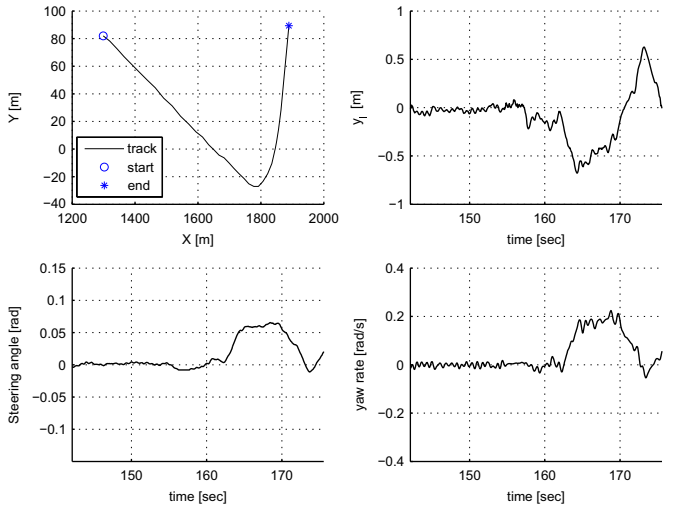

Fig. 12. Demanding path following maneuvre performed by the Peugeot 307 on the test track ($v \in [15-16.5]$ m/s).

6. Conclusions

A vision based lane keeping control for autonomous vehicles has been proposed, simulated and experimentally tested providing both lane keeping and yaw rate stabilization at the same time on the basis of yaw rate and lateral offset measurements only. As a first step, on the basis of lateral displacements at a look-ahead distance provided by a vision system, a reference yaw rate signal is designed using PID control techniques with a double integral action. As a second step the steering angle is designed as a PI control based on the yaw rate tracking error following well established active steering design. A multivariable control problem (two outputs, one input) has been solved via two independent PID nested loops. The robustness of the proposed control with respect to speed variations, look-ahead distance and parameter uncertainties such as mass, front and rear cornering stiffnesses has been theoretically analyzed. Simulations in the CarSim environment illustrate the performance achieved by the proposed lane keeping control strategy both on a standard path and during a μ-split braking maneuvre. The proposed controller is compared by simulation with the MPC used in CarSim as steering control which also requires the vehicle lateral speed and orientation: a reduced lateral offset and new stable μ-split braking maneuvres are obtained by the proposed controller. The experimental test, performed by a Peugeot 307 prototype vehicle on the test track in Satory, 20 km west of Paris, successfully validates the controller; tests are performed both for straight lines and curves and show good performance. Future work will explore the interactions of the proposed controller with the driver both during normal driving and in emergency conditions.

Acknowledgments

The authors would like to thank the experimental group in LIVIC (Vehicle-Infrastructure-Driver Interactions Research Unit) for their help and support in making the in-vehicle implementation possible.

References

Ackermann, J. (2002). *Robust control*. London: Springer.

Ackermann, J., Sienel, J., Steinhauser, R., & Utkin, V. I. (1995). Linear and nonlinear controller design for robust automatic steering. *IEEE Transactions on Control Systems Technology*, *3*(1), 132–143.

Baumgarten, G. (2004). *Motor vehicle steering system having a yaw rate controller*, *Bayerische Motoren Werke*, United States Patent Pub. No. US 20040070268, April 15/2004.

Broggi, A., Bertozzi, M., Fascioli, A., Lo Bianco, C. G., & Piazzi, A. (1999). The ARGO autonomous vehicle's vision and control systems. *International Journal of Intelligent Control and Systems*, *3*(4), 409–441.

Cerone, V., Chinu, A., & Regruto, D. (2002). Experimental results in vision-based lane keeping for highway vehicles. In *Proceedings of the American control conference*, Anchorage, AK, May 8–10.

Cerone, V., Milanese, M., & Regruto, D. (2009). Combined automatic lane keeping and driver's steering through a 2-dof control strategy. *IEEE Transactions on Control Systems Technology*, *17*(1), 135–142.

Enache, N. M., Mammar, S., & Netto, M. (2008). Driver steering assistance for lane departure avoidance based on hybrid automata and on composite lyapunov function. *IEEE Transactions on Intelligent Transportation Systems*, *11*(1).

Enache, N. M., Netto, M., Mammar, S., & Lusetti, B. (2009). Driver steering assistance for lane departure avoidance. *Control Engineering Practice*, *17*(6), 642–651.

Falcone, P., Borrelli, F., Asgari, J., Tseng, H. E., & Hrovat, D. (2007). Predictive active steering control for autonomous vehicle systems. *IEEE Transactions on Control Systems Technology*, *15*(3), 566–580.

Foote, T. B., Cremean, L. B., Gillula, J. H., Hines, G. H., Kogan, D., & Kriechbaum, K. L., et al. (2006). Alice: An information-rich autonomous vehicle for high-speed desert navigation. *Journal of Field Robotics*, *23*(9), 777–810.

Gill, P. E., Murray, W., & Wright, M. H. (1981). *Practical optimization*. London, UK: Academic Press.

Grassi, E., Tsakalis, K. S., Dash, S., Gaikwad, S. V., MacArthur, W., & Stein, G. (2001). Integrated system identification and PID controller tuning by frequency loop-shaping. *IEEE Transactions on Control Systems Technology*, *9*(2), 285–294.

Hatipoglu, C., Redmill, K., & Özgüner, Ü. (1997). Steering and lane change: A working system. In *IEEE conference on intelligent transportation systems* (pp. 272–277), Boston, MA.

Kang, J., Hindiyeh, R. Y., Moon, S., Gerdes, J. C., & Yi, K. (2008). Design and testing of a controller for autonomous vehicle path tracking using GPS/INS sensors. In *Proceedings of the 17th IFAC World congress*, Seoul, Korea, July 6–11.

Labayrade, R., Douret, J., Laneurit, J., & Chapuis, R. (2006). A reliable and robust lane detection system based on the parallel use of three algorithms for driving safety assistance. *IEICE Transactions on Information and Systems*, *E89-D*(7), 2092–2100.

Labayrade, R., Ieng, S. S., & Aubert, D. (2004). A reliable road lane detector approach combining two vision-based algorithms. In *IEEE intelligent transportation systems conference*, Washington, DC, USA, October 3–6.

Liu, L., Nagai, M., & Raksincharoensak, P. (2008). On torque control of vehicle handling and steering feel for avoidance maneuver with electric power steering. In *Proceedings of the 17th IFAC World congress*, Seoul, Korea, July 6–11.

MacAdam, C. C. (1981). Application of an optimal preview control for simulation of closed-loop automobile driving. *IEEE Transactions on Systems, Man, and Cybernetics*, *11*, 393–399.

Marino, R., Scalzi, S., Netto, M., & Orlando, G. (2009). A nested PID steering control for lane keeping in vision based autonomous vehicles. In *American control conference*, St. Louis, Missouri, USA, June 10–12.

Montemerlo, M., Thrun, S., Dahlkamp, H., Stavens, D., Aron, A., & Diebel, J., et al. (2006). Stanley: The robot that won the DARPA grand challenge. *Journal of Field Robotics*, *23*(9), 661–692.

Pacejka, H. B. (2004). *Tire and vehicle dynamics*. Elsevier, Butterworth Heinemann.

Paoletti, S., Grasselli, O. M., & Menini, L. (2004). A comparison between classical robust stability conditions. *International Journal Robust and Nonlinear Control*, *14*, 249–271.

Pauly, A., & Baumgarten, G. (2005). *Overlay steering system and method for motor vehicles*, *Bayerische Motoren Werke*, United States Patent Pub. No. US 6854558, February 15/2005.

Raharijaona, T., Duc, G., & Mammar, S. (2004). H_∞ controller synthesis and analysis with application to lateral driving assistance. In *IFAC symposium on advance in automotive control*, Salerno, Italy, April.

Shladover, S. E. (2007). PATH at 20—history and major milestones. *IEEE Transactions on Intelligent Transportation Systems*, *8*(4).

Takahashi, A., & Asanuma, N. (2000). Introduction of HONDA ASV-2 (advanced safety vehicle-phase 2). In *Proceedings of the IEEE intelligent vehicles symposium*, Dearborn, MI, USA, October 3–5.

Urmson, C., Duggins, D., Jochem, T., Pomerleau, D., & Thorpe, C. (2008). From automated highways to urban challenges. In *Proceedings of the 2008 IEEE international conference on vehicular electronics and safety*, Columbus, OH, USA, September 22–24, 2008.

Vidyasagar, M., & Kimura, H. (1986). Robust controllers for uncertain linear multivariable systems. *Automatica*, *22*(1), 85–94.